

## A statistical mechanical theory for a two-dimensional model of water

Tomaz Urbic<sup>1,a)</sup> and Ken A. Dill<sup>2</sup><sup>1</sup>*Faculty of Chemistry and Chemical Technology, University of Ljubljana, Aškerčeva 5, 1000 Ljubljana, Slovenia*<sup>2</sup>*Department of Pharmaceutical Chemistry, University of California, San Francisco, California 94143-1204, USA*

(Received 27 November 2009; accepted 24 May 2010; published online 14 June 2010)

We develop a statistical mechanical model for the thermal and volumetric properties of waterlike fluids. Each water molecule is a two-dimensional disk with three hydrogen-bonding arms. Each water interacts with neighboring waters through a van der Waals interaction and an orientation-dependent hydrogen-bonding interaction. This model, which is largely analytical, is a variant of the Truskett and Dill (TD) treatment of the “Mercedes-Benz” (MB) model. The present model gives better predictions than TD for hydrogen-bond populations in liquid water by distinguishing strong cooperative hydrogen bonds from weaker ones. We explore properties versus temperature  $T$  and pressure  $p$ . We find that the volumetric and thermal properties follow the same trends with  $T$  as real water and are in good general agreement with Monte Carlo simulations of MB water, including the density anomaly, the minimum in the isothermal compressibility, and the decreased number of hydrogen bonds for increasing temperature. The model reproduces that pressure squeezes out water’s heat capacity and leads to a negative thermal expansion coefficient at low temperatures. In terms of water structuring, the variance in hydrogen-bonding angles increases with both  $T$  and  $p$ , while the variance in water density increases with  $T$  but decreases with  $p$ . Hydrogen bonding is an energy storage mechanism that leads to water’s large heat capacity (for its size) and to the fragility in its cagelike structures, which are easily melted by temperature and pressure to a more van der Waals-like liquid state. © 2010 American Institute of Physics. [doi:10.1063/1.3454193]

### I. INTRODUCTION

We describe here a simple model of water’s volumetric and thermal properties, including its anomalous behaviors. On the one hand, there is a long and rich history of modeling pure water, including Röntgen’s two-density model in 1897,<sup>1</sup> Pople’s 1951 model of the bending of hydrogen bonds in a tetrahedral lattice,<sup>2</sup> lattice and cluster models,<sup>3–13</sup> treatments of water’s unusual density behavior using double-well spherically symmetric potentials,<sup>14–17</sup> and treatments that begin with water’s pair-correlation function or experimentally measured moments of distribution functions in place of a molecular potential.<sup>18–20</sup> In addition, there have been many computer simulations<sup>21–23</sup> including those based on multi-point classical force-field models such as simple point charge (SPC) and transferable intermolecular potential (TIP),<sup>24–28</sup> or polarizable versions of them,<sup>29–32</sup> or quantum-mechanical treatments.<sup>33–35</sup> We will not review this large literature here as this was done before.<sup>36–40</sup>

On the other hand, despite this remarkable and extensive body of work, water is not yet fully understood. Integral equations and other methods of liquid state theory led to a fairly detailed understanding of Lennard-Jones (LJ) liquids, such as argon, which are governed by spherically symmetric potentials, and of dipolar liquids, such as acetonitrile or nitroethane, which are governed by dipolar or Stockmayer po-

tentials. Dipoles have relatively simple orientational interactions.<sup>41</sup> However, water is more difficult to model because its hydrogen-bonding arms, which are the source of water’s orientation-dependent interactions, are coupled to each other rigidly and sterically (i.e., in an approximation to reduce the number of degrees of freedom of the model we can say when a water molecule rotates, moving one hydrogen-bonding arm, it rigidly moves all the other hydrogen-bonding arms). This rigid internal orientational coupling of interactions leads to complex angular effects that are multibody and nonlocal (a water molecule connects with other waters through networks, causing orientational correlations out to third and more distant neighbors), and such effects have been notoriously hard to treat. Hence, it has been challenging to develop analytical theories.<sup>5,42–44</sup> So, water is often studied by computer simulations, but they are expensive. Because of the large amount of computational sampling required, it is challenging, using quantum-mechanical or atomically detailed computer simulations,<sup>45–47</sup> to explore water’s entropies or heat capacities or effects of pressure or water’s pressure-temperature phase diagram (see Refs. 45 and 48–50 for exceptions). Some of the models have, however, been extended to even heavy water with apparently quite reasonable success.<sup>51</sup>

Here, our aim is to develop a statistical mechanical model: (1) that treats approximately the balance between LJ interactions, on the one hand, and orientational hydrogen-bonding interactions on the other hand, (2) that is sufficiently

<sup>a)</sup>Electronic mail: tomaz.urbic@fkt.uni-lj.si.

simple that we can obtain full entropies, heat capacities, and thermal and volumetric properties and their variances without sampling limitations, and (3) that is analytical so that it can be studied without large computational resources. Our model is intended to capture qualitative trends, not quantitative detail. Because it is analytical, it may be useful in the same way that the van der Waal (vdW) gas model gives basic insights.

Our model is two dimensional (2D). It is a variant of the so-called Mercedes-Benz (MB) model, so named because each water is a disk with three hydrogen-bonding arms, resembling the MB logo. The MB model, originally proposed by Ben-Naim<sup>52,53</sup> in 1971, has been studied extensively by ( $N, p, T$ ) Monte Carlo simulations<sup>54–59</sup> and by integral equation methods<sup>60–65</sup> based on Wertheim’s theory for associating fluids.<sup>66,67</sup> The MB model of water was recently extended to three dimensions (3D) by our group<sup>68,69</sup> and Dias *et al.*<sup>70</sup> In particular, our treatment here is most directly descendant from a treatment of Truskett and Dill,<sup>71–73</sup> who developed a nearly analytical version of the MB model. The present work differs from the Truskett and Dill (TD) model in that (1) the present treatment is simpler, relying only on two-body terms for the liquid state. (2) We treat ice as having higher multi-body cooperativity, in a way that we believe is more realistic. (3) We make here direct tests against the underlying MB model, which has been studied by Monte Carlo simulations. (4) Our study is now much broader, we also study the effects of pressure and we compute the variances of hydrogen-bond angles and packing densities; we find them to be in qualitative agreement with earlier work of Henn and Kauzmann.<sup>74</sup> (5) Our derivation is now simpler and more intuitive for the full system partition function. (6) Also, we find that the new model gives better predictions for the numbers of hydrogen bonds versus temperature, more in line with experiments, than the earlier TD treatment. The virtues of a 2D model are that: (a) to the extent that it captures properties of real water, it illuminates what details of structure and geometry are not essential for explaining water physics, and (b) the water structures that give rise to the physical properties are easier to visualize. We believe that the present approach will be readily generalizable to 3D to new MB model and to reproduce experimental water data.

## II. THEORY

We consider a system of  $N$  water molecules. For the purpose of keeping track of the state of interaction of each possible hydrogen-bonding arm of each water molecule, we use as a bookkeeping tool an underlying ice lattice. For this 2D threefold symmetric water model, the underlying lattice is hexagonal; see Fig. 1. Focus on a single water molecule in the hexagon and the relationship of that water to its clockwise neighbor. Figure 2 shows the three possible relationships: The test water either forms a hydrogen bond, it forms a vdW contact, or it forms no interaction at all, either because the adjacent site is empty or because the adjacent water is too distant from the test water. We aim to compute the isothermal-isobaric statistical weights,  $\Delta_{\text{HB}}$  of the hydrogen-

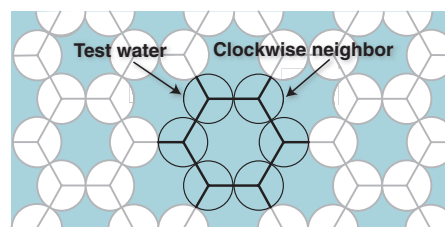


FIG. 1. The lattice of the model showing both the hexagon of the icelike structure and showing illustrating a pair interaction used for bookkeeping to avoid triple counting.

bonded molecules,  $\Delta_{\text{LJ}}$  of the vdW contacts, and  $\Delta_o$  of the unbonded population as functions of temperature, pressure, and interaction energies.

### A. The hydrogen-bonded state

First, here is how we represent the hydrogen-bonded state and its Boltzmann factor. We assume that if the test water molecule points one of its three hydrogen-bonding arms at an angle  $\theta$  to within  $\pi/3$  of the center of its clockwise neighbor water, it forms a hydrogen bond (see Fig. 2). The energy of interaction of the test water with its clockwise neighbor is

$$u_{\text{HB}}(\theta) = -\epsilon_{\text{HB}} - \epsilon_{\text{LJ}} + k_s \theta^2, \quad -\pi/3 < \theta < \pi/3, \quad (1)$$

where  $\epsilon_{\text{HB}}$  is an energy constant representing the maximal strength of a hydrogen bond.  $\epsilon_{\text{LJ}}$  is the contact energy between neighboring waters (this component was handled differently, and not included in this term, in the original model of Truskett and Dill<sup>71,72</sup>), and  $k_s$  is the angular spring constant that describes the weakening of the hydrogen bond as it

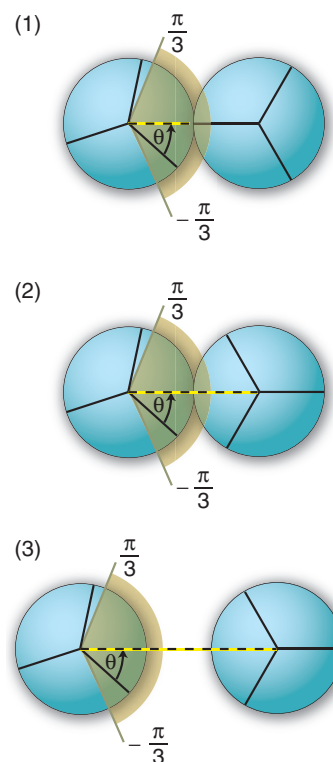


FIG. 2. The three model states: (1) hydrogen bonded, (2) vdW bonded, and (3) nonbonded.

becomes increasingly off angle. We regard this type of hydrogen bond as weak insofar as it is not cooperative with neighboring hydrogen bonds. We consider a more cooperative type of hydrogen bonding below. To compute the isothermal-isobaric partition function,  $\Delta_{\text{HB}}$ , of this hydrogen-bonded state, we integrate this Boltzmann factor over all the allowable angles and over all the allowable separations  $x$  and  $y$  of the test molecule relative to its clockwise neighbor,

$$\Delta_{\text{HB}} = c(T) \iint dx dy \int_{-\pi/3}^{\pi/3} d\theta \times \exp(- (u_{\text{HB}} + 2pv_{\text{HB}}/3)/k_B T), \quad (2)$$

where  $c(T)$  is the 2D version of the kinetic energy contribution to the partition function,  $k_B$  is Boltzmann's constant,  $T$  is temperature,  $p$  is the pressure, and  $v_{\text{HB}}$  is volume per molecule (in this 2D model, it is actually an area, but we retain the pressure-volume terminology for later comparisons with experiments). The double integral  $\iint dx dy$  represents the volume over which the second molecule has translational freedom to form a hydrogen bond with the first water and is equal to effective volume  $v_{\text{ef}}^{\text{HB}}$ . This is calculated from original MB potential.

Here is how we determine the volume  $v_{\text{HB}}$  of the hydrogen-bonded state. First, we estimate an upper bound on the volume, from a simple geometric calculation. For the perfect hexagon crystal, representing low-pressure ice, the volume of the solid is

$$v_s = \frac{3\sqrt{3}r_{\text{HB}}^2}{4}, \quad (3)$$

provided the center of the hexagon is unoccupied, as in our current model,  $r_{\text{HB}}$  is the distance of strongest hydrogen bond same as in original MB model<sup>55</sup> [we use Eq. (3) to get the volume per molecule of ice; see below.] Second, since liquid water is denser than ice, we estimate a lower bound on the volume using high-pressure ice, where another MB water occupies the center of each hexagonal cage,<sup>71</sup>

$$v_{\text{HB}}^{\text{hp}} = \frac{\sqrt{3}r_{\text{HB}}^2}{2}. \quad (4)$$

Finally, since the density of liquid water must lie between these limits, we estimate its volume as

$$v_{\text{HB}} = \frac{\sqrt{3}r_{\text{HB}}^2 x_v}{2}, \quad (5)$$

where  $x_v = 1.1$  is simply chosen empirically by fitting the density dependence versus temperature. In this way, our liquid water is 10% less dense than the maximally packed structure.

Using these definitions and performing the integration in Eq. (2) gives

$$\Delta_{\text{HB}} = c(T) v_{\text{ef}}^{\text{HB}} \exp\left(\frac{\epsilon_{\text{HB}} + \epsilon_{\text{LJ}} - 2pv_{\text{HB}}/3}{k_B T}\right) \times \sqrt{\frac{k_B T \pi}{k_s}} \operatorname{erf}\left(\sqrt{\frac{k_s \pi^2}{9k_B T}}\right). \quad (6)$$

## B. The vdW state

In the second possible state, the test water molecule forms a vdW contact with its clockwise neighboring water, but it forms no hydrogen bond. This type of water molecule has energy

$$u_{\text{LJ}} = -\epsilon_{\text{LJ}}, \quad (7)$$

where  $\epsilon_{\text{LJ}}$  is the same as described above. The isothermal-isobaric partition function,  $\Delta_{\text{LJ}}$  of this state is given by integrating over angles and positions of the test particle relative to its clockwise neighbor,

$$\Delta_{\text{LJ}} = c(T) \iint dx dy \int_{-\pi/3}^{\pi/3} d\theta \times \exp(- (u_{\text{LJ}} + 2pv_{\text{LJ}}/3)/k_B T), \quad (8)$$

where we take the volume occupied by the test water in this state to be

$$v_{\text{LJ}} = \frac{\sigma_{\text{LJ}}^2 \sqrt{3} \sqrt{2}}{2}. \quad (9)$$

The integral  $\iint dx dy$  represents the translation volume when second molecule forms vdW contact with first and is equal to effective volume  $v_{\text{ef}}^{\text{LJ}}$  and  $\sigma_{\text{LJ}}$  is the vdW contact distance of MB molecules (see original potential). Integrating gives

$$\Delta_{\text{LJ}} = \frac{2\pi}{3} c(T) v_{\text{ef}}^{\text{LJ}} \exp\left(\frac{\epsilon_{\text{LJ}} - 2pv_{\text{LJ}}/3}{k_B T}\right). \quad (10)$$

## C. The noninteracting state

In this third possible state, the test water has no interaction with its clockwise neighbor, so the energy is

$$u_o(\theta) = 0. \quad (11)$$

The isothermal-isobaric partition function for the noninteracting state is obtained by integrating over translational degrees of freedom,

$$\Delta_o = c(T) \iint dx dy \int_{-\pi/3}^{\pi/3} d\theta \exp(- 2pv_o/3k_B T), \quad (12)$$

where  $v_o$  is volume available to the test molecule in this state. Following Refs. 71 and 72, we compute  $v_o$  using the vdW gas approximation,

$$v_o = \frac{k_B T}{p} + v_{\text{LJ}}. \quad (13)$$

Integrating over all the ways this state can occur gives

$$\Delta_o = \frac{2\pi}{3} c(T) \frac{k_B T}{p} \exp\left(\frac{- 2pv_o}{3k_B T}\right). \quad (14)$$

These three expressions, Eqs. (6), (10), and (14), give the isobaric-isothermal ensemble Boltzmann weights of the three possible states of each water molecule: hydrogen bonded, vdW bonded, or nonbonded. Following Truskett and Dill,<sup>71,72</sup> we assume a mean-field attractive energy,<sup>75</sup>  $-Na/v$ ,

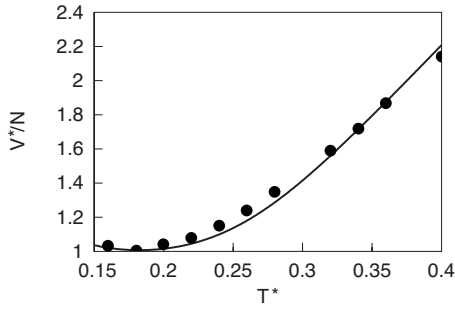


FIG. 3. Temperature dependence of the molar volume at  $p^*=0.19$ . Theory (line) vs the Monte Carlo simulation of the MB model (Ref. 55) (symbols).

beyond pair interactions, where  $a$  is the vdW dispersion parameter (0.02, here) and  $v$  is the average molar volume, which we get from Eq. (20) below.

### III. STATISTICAL MECHANICS OF THE MODEL

Now, once the energy parameters of the model are given, the partition function for a full hexagon of six waters would be given by

$$Q_1 = (\Delta_{\text{HB}} + \Delta_{\text{LJ}} + \Delta_o)^6, \quad (15)$$

where subscript 1 indicates a single hexagon. However, we treat hexagons here a little differently instead. We believe that true ice cages in water's solid states involve a higher degree of hydrogen-bonding cooperativity than the hydrogen bonding that is just formed pairwise among nearest neighbor waters in the liquid state. So, for ice, throughout this paper, the total partition function for each hexagon will be given by

$$Q_1 = (\Delta_{\text{HB}} + \Delta_{\text{LJ}} + \Delta_o)^6 - \Delta_{\text{HB}}^6 + \delta\Delta_s^6, \quad (16)$$

where  $\delta = \exp(-\beta\epsilon_c)$  is the Boltzmann factor for the cooperativity energy  $\epsilon_c$  that applies only when six water molecules all collect together into a full hexagonal cage. The terms on the right side of this expression simply replace the statistical weight for each weakly hydrogen-bonded full hexagonal cage with the statistical weight for a cooperative strongly hydrogen-bonded hexagonal cage.  $\Delta_s$  is the Boltzmann factor for a cooperative hexagonal cage. It differs from  $\Delta_{\text{HB}}$  only in that the former uses the hexagonal cage volume per molecule,  $v_s$ , while the latter uses the liquid water hydrogen-bonding volume per molecule,  $v_{\text{HB}}$ . We use Eq. (16) for the full range of temperatures; it reduces to Eq. (15) in the limit of high temperatures when all cagelike structuring of water

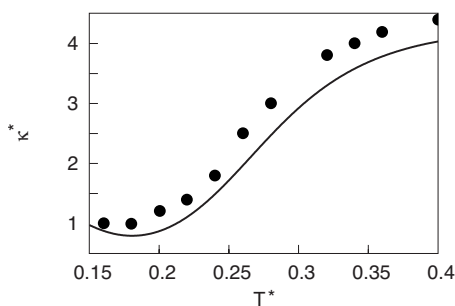


FIG. 4. Temperature dependence of the isothermal compressibility; legend otherwise as for Fig. 3.

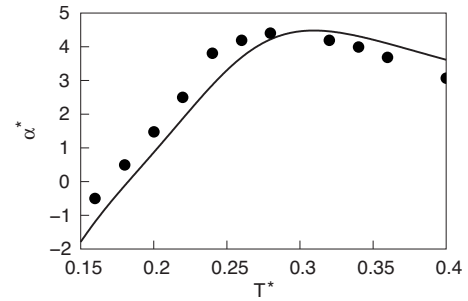


FIG. 5. Temperature dependence of the thermal expansion coefficient; legend otherwise as for Fig. 3.

has disappeared. Now we combine the Boltzmann factors for the individual water molecules to get the partition function  $Q$  for the whole system of  $N$  particles,

$$Q = Q_1^{N/6}, \quad (17)$$

where the factor  $N/6$  accounts for the three possible interaction sites per water molecule, and corrects for double counting the hydrogen bonds.

We compute the populations of the states  $i=1$  (HB), 2 (LJ), 3 (o), and 4 (solid) using

$$f_i = \frac{d \log Q_1}{d \log \Delta_i}. \quad (18)$$

The chemical potential is given by

$$\mu = -\frac{k_B T}{N} \log Q. \quad (19)$$

The molar volume is

$$v = \frac{V}{N} = \left( \frac{\partial \mu}{\partial p} \right)_T = \sum f_i v_i, \quad (20)$$

and all the other thermodynamic properties below are obtained as described previously.<sup>71,72</sup>

### IV. RESULTS AND DISCUSSION

For all the model calculations below, we used the following parameters:  $\epsilon_{\text{HB}}=1$ ,  $r_{\text{HB}}=1$ , vdW:  $\epsilon_{\text{LJ}}=0.1$ ,  $\sigma_{\text{LJ}}=0.7$  [unchanged from TD (Refs. 71 and 72) and MB models<sup>55</sup>],  $k_s=10$ , and  $\epsilon_c=0.06$ . To get a sense for these numbers, a typical hydrogen bond in the gas phase has a bond energy of about 20 kJ/mol found experimentally. So the cooperativity energy in our model is very small, 1% of that value, per mole of hexagons, or about 0.2 kJ/mol per hydrogen bond. Small changes in cooperativity energy do not affect results. We present our results below in dimensionless units, normalized to the strength of the optimal hydrogen bond  $\epsilon_{\text{HB}}$  and hydrogen bond separation  $r_{\text{HB}}$ . ( $T^*=k_B T/|\epsilon_{\text{HB}}|$ ,  $u^{\text{ex}}=u^{\text{ex}}/|\epsilon_{\text{HB}}|$ ,  $V^*=V/r_{\text{HB}}^2$ , and  $p^*=pr_{\text{HB}}^2/|\epsilon_{\text{HB}}|$ ). We would also like to state that potential between two molecule in simulations is not the same as in theory due to approximations made. All distance dependent parts are fit into effective volumes.

Figure 3 compares predictions of present theory for the molar volume,  $V^*/N$  of water, to NPT Monte Carlo simulations<sup>55</sup> of the MB model with the same parameters. The calculations were performed at a reduced pressure of

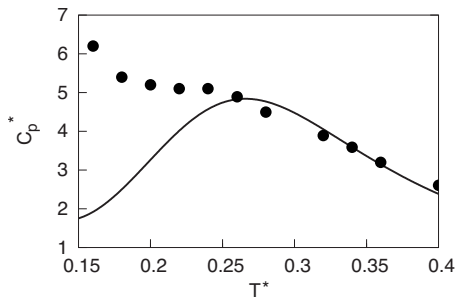


FIG. 6. Temperature dependence of the heat capacity at constant pressure; legend otherwise as for Fig. 3.

$p^*=0.19$ . The theory is in good general agreement with the simulations, including the density maximum, although the theory reproduces a density max that is slightly shifted ( $T^*=0.1825$ ) relative to the simulations ( $T^*=0.18$ ). This may be either because of approximations in the theory, or because even though the theory is modeled roughly on the MB model, the theory does not have exactly the same underlying Hamiltonian, so it should not be expected to give exactly the same results.

Figures 4–6 show the temperature dependences of the isothermal compressibility,  $\kappa_T^*$ , the thermal expansion coefficient,  $\alpha^*$ , and the heat capacity,  $C_p^*$ , respectively. We do not show the properties of the ice phase or of the liquid-to-solid phase transition here. Rather, we show the properties of the model that aim to capture the liquid state, which becomes the supercooled state at low temperatures. For these quantities too, the theory generally reproduces well the Monte Carlo results. However, while the Monte Carlo simulations of the MB water show a minimum in the isothermal compressibility versus temperature, it is not as pronounced as in experiments.<sup>55</sup> The present theory also reproduces a minimum in  $\kappa_T^*$  (Fig. 6), consistent with scattering experiments.<sup>76</sup> At low temperatures, our present model shows a drop in  $C_p$  as the temperature is reduced, whereas the MB model does not. We think that this is a consequence of the water-cage cooperativity that we have included here, which was not included in the MB model. Because we believe this small cooperativity upon cage formation is real, we believe that this shows a limitation of the original MB model, rather than of the theory, in this case.

Figure 7 shows the fraction of hydrogen bonds that are broken as a function of temperature. Results are shown for a reduced pressure of  $p^*=0.19$ . In the earlier TD model, the

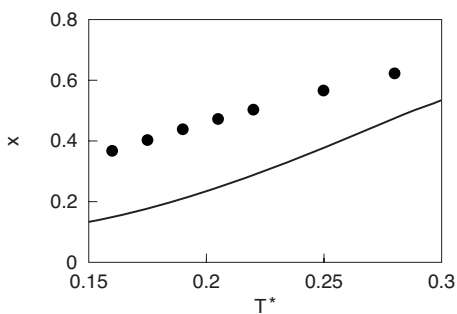


FIG. 7. Temperature dependence of the fraction  $x$  of hydrogen bonds that are broken; legend otherwise as for Fig. 3.

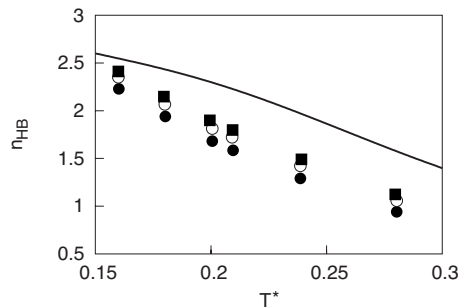


FIG. 8. Temperature dependence of the average number,  $n_{\text{HB}}$ , of hydrogen bonds (theory, line), compared to Monte Carlo MB simulations (Ref. 55) for different cutoffs [the cutoffs are 0.5 (filled circles), 0.4 (empty circles), and 0.25 (filled squares)].

fraction of hydrogen bonds made in the liquid state was considerably lower than is seen in experiments. The present theory gives much better agreement with both experiments and with the Monte Carlo MB simulation results.<sup>55</sup> Even so, the agreement is not perfect. The theory still underpredicts hydrogen bonding compared to the MB simulations. However, we believe this is for the trivial reason that the MB simulations use a tighter definition for the range of angles that define a hydrogen bond. Figure 8 shows a related quantity, the average number of hydrogen bonds made per water molecule versus temperature. We plotted computer simulations for different cutoffs [the cutoffs are 0.5 (filled circles), 0.4 (empty circles), and 0.25 (filled squares)]. The present theory overestimates the number of hydrogen bonds, more so at higher temperatures. The shape of the curve is consistent with results of Sastry<sup>42</sup> and Franzese.<sup>77</sup> In our theory we

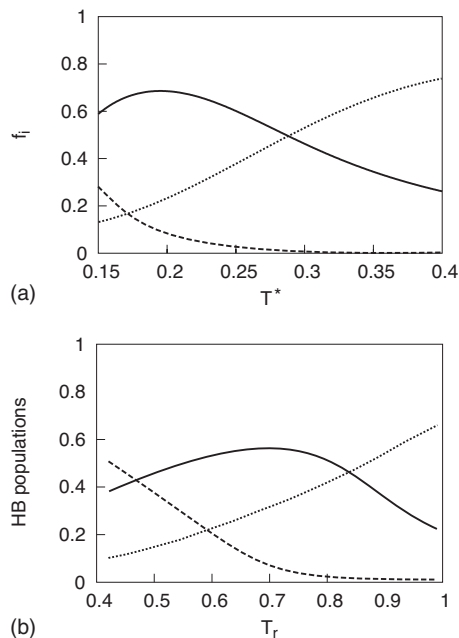


FIG. 9. (a) Temperature dependence of the populations  $f_i$  of the different type of hydrogen bonds, at constant pressure,  $p^*=0.19$ . The population of strong hydrogen bonds (long dashed line), weak hydrogen bonds (solid line), and no hydrogen bonds (short dashed line). (b) Experimental populations of OH states in liquid water vs temperature  $T_r$  (Ref. 71) along its saturation curve, from IR spectroscopic data [adapted from Fig. 5 of Luck (Ref. 78)]. Temperature here  $T_r$  is reduced to critical temperature.

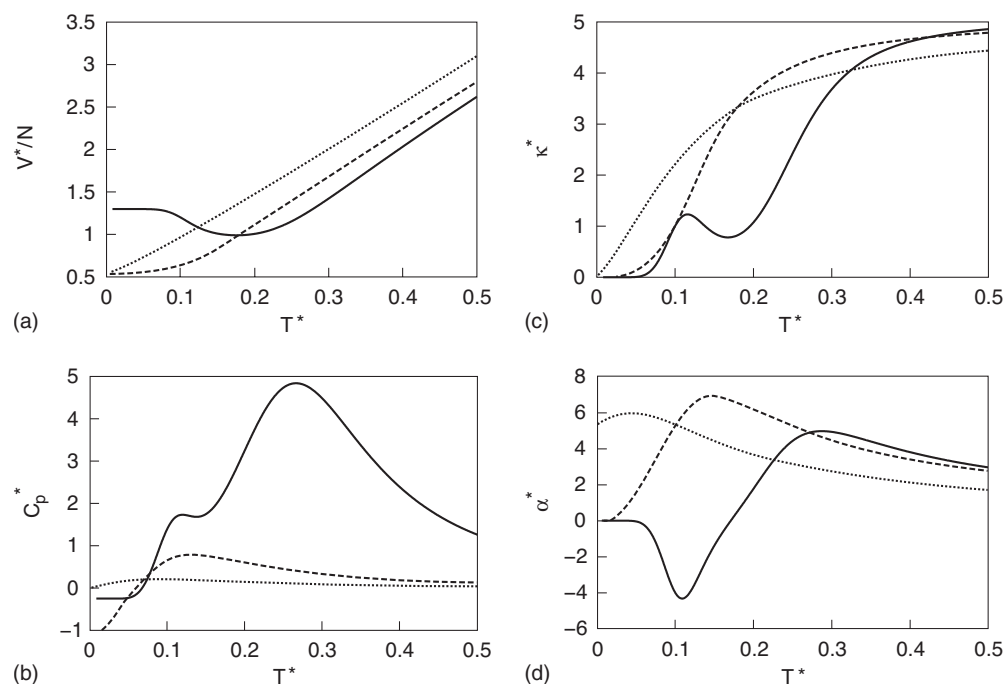


FIG. 10. Temperature dependence of the molar volume (a), heat capacity (b), isothermal compressibility (c), and thermal expansion coefficient (d) at  $p^* = 0.19$ : theory (solid line), LJ disks (long dashed line), and vdW 2D gas (dashed line).

have all molecules forming hydrogen bonds at low temperatures while at high temperature there is almost no hydrogen bond.

Figure 9(a) shows the model populations of the strong hydrogen-bonding state, weak hydrogen-bonding state, and the state of no hydrogen bonds versus temperature, indicating the melting out of strong hydrogen bonding with temperature and the melting out of weak hydrogen-bonding interactions at higher temperatures. Figure 9(b) shows

corresponding experimental data for the populations of strong and weak hydrogen bonds as measured from OH stretching bands in IR spectroscopy by Luck.<sup>78</sup> Luck identifies three spectroscopic states: strongly cooperative hydrogen bonded, weakly cooperative hydrogen bonded, and non-bonded. We regard these three states as corresponding to the three states in our theory. Qualitatively, the trends are the same, but there is no quantitative agreement. Strong hydrogen bonds are prevalent in cold water and are important also

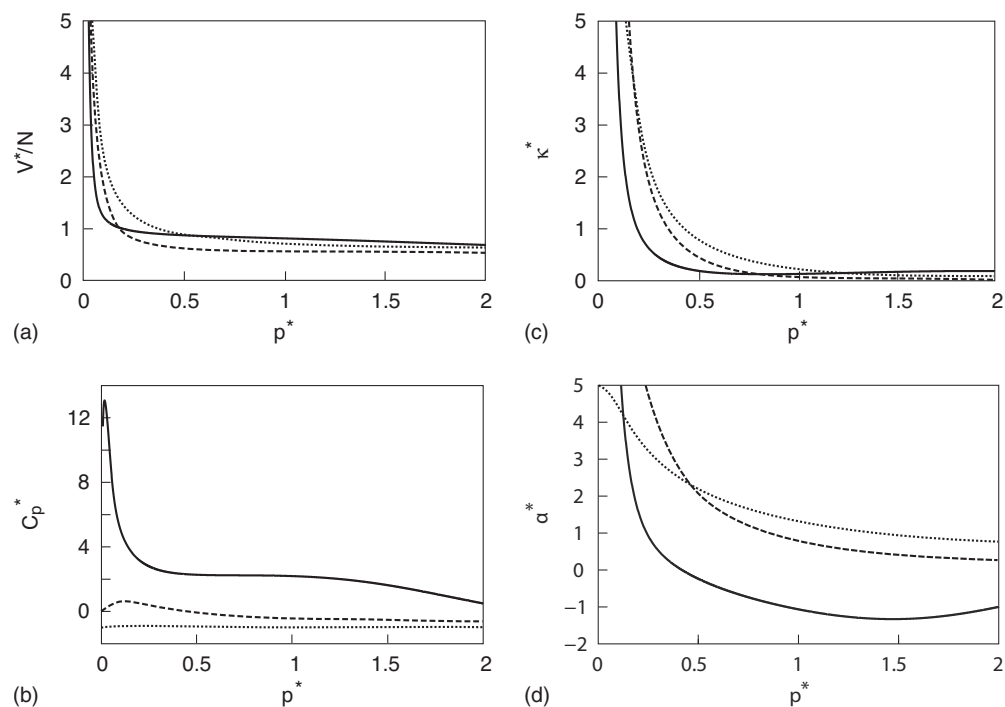


FIG. 11. Pressure dependence of the molar volume (a), heat capacity (b), isothermal compressibility (c), and thermal expansion coefficient (d) at  $T^* = 0.20$ : theory (solid line), LJ disks (long dashed line), and vdW 2D gas (dashed line).

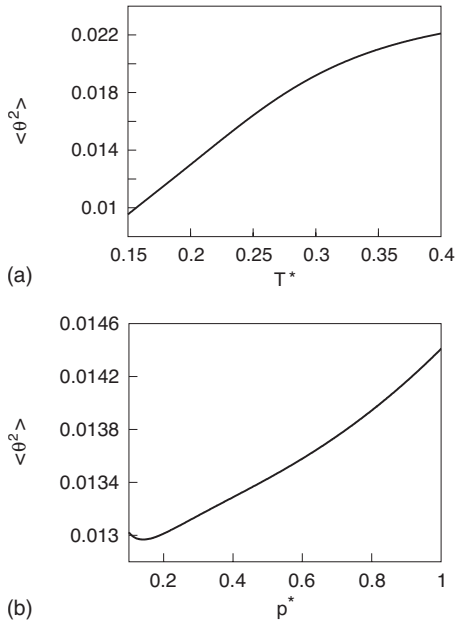


FIG. 12. (a) Temperature dependence of variance of the hydrogen-bond angle,  $\langle \theta^2 \rangle$  at constant pressure,  $p^* = 0.19$ . (b) Pressure dependence of the  $\langle \theta^2 \rangle$  at constant temperature,  $T^* = 0.20$ .

in case of solvation. Heating melts the strong HB structures into structures that have a mixture of weak hydrogen bonds, LJ interactions, and nonbonded structures at intermediate temperatures. At higher temperatures, approaching the critical point, the weak hydrogen bonds break to form nonbonded gas-phase states.

We are also interested in the pressure dependences of various properties of model water. No studies have been performed, as far as we know, of the pressure dependences of properties in the MB model. Also, there are few experimental studies on water of pressure dependences at fixed tempera-

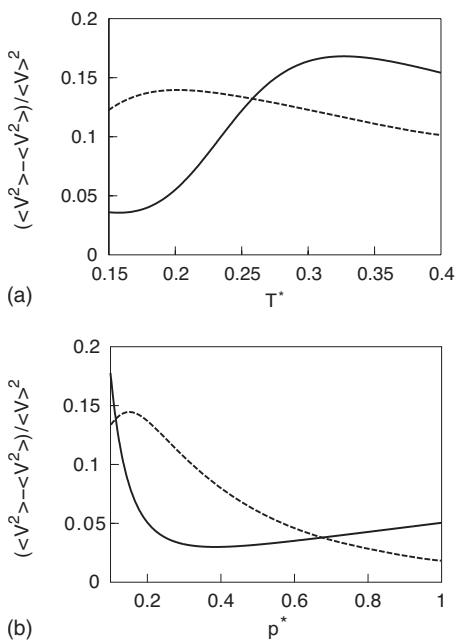


FIG. 13. (a) Temperature dependence of the variance of volume at constant pressure,  $p^* = 0.19$ , and (b) at constant temperature,  $T^* = 0.20$  for the MB model (solid line) and LJ disks (dashed line).

ture of the volumetric and thermal properties.<sup>79,80</sup> So, Figs. 10 and 11 compare the temperature and pressure dependences of the molar volume, isothermal compressibility,  $\kappa_T^*$ , the thermal expansion coefficient,  $\alpha^*$ , and the heat capacity,  $C_p^*$ , from our water model to two models that are intended to describe simpler liquids: the vdW equation for a 2D gas and the present model with the hydrogen bonds turned off, to mimic a LJ-like liquid. For the latter, we set  $u_{\text{HB}}(\theta) = \infty$ .

Two interesting results are shown in Fig. 11. First, relatively small pressures appear to “melt out” much of the heat capacity, presumably the most cagelike low-density hydrogen-bonding component. Second, the model predicts that pressure drives water into a state of negative thermal expansion, such as is found in a very narrow range of temperatures in very cold liquid water at  $p = 1$  atm. These two properties are likely related to each other. This is presumably the state of water in which heating melts out hydrogen bonding, driving the system to a denser state. Otherwise, pressure affects water much like it affects vdW liquids. For example, the adiabatic compressibility of liquid argon monotonically decreases with pressure.<sup>81</sup> The vdW model also shows some increase of heat capacity with pressure at low pressures, then decreasing, consistent with experiments on carbon dioxide and argon between 323 and 423 K and at pressures up to 25 MPa.<sup>82</sup>

Figure 12 shows temperature and pressure dependences of the second moment  $\langle \theta^2 \rangle$  of the hydrogen-bond angles in water. Increasing the temperature or pressure bends the water-water hydrogen bonds, broadening the distribution of angles as the system varies at low temperatures and pressures from being highly water-cage-like to being more vdW-like. The small exception is at low pressures, where increasing pressure causes water to become more structured.

Figure 13 shows the variance of the volume in the water model and LJ disks. Interestingly, these volumetric fluctuations are predicted to be quite different in water than in simpler fluids. Water’s volumetric fluctuations are small in cold cagelike water and melted out at higher temperatures. Similarly, pressure squeezes the fluctuating cages into a denser vdW-like state that fluctuates less. The general trends in Figs. 12 and 13 are consistent with an earlier model of Henn and Kauzmann.<sup>83</sup>

## V. CONCLUSIONS

We described here a simple 2D model for the thermal and volumetric properties of water. The model assumes three macrostates for each water-water interaction: hydrogen bonded, or vdW bonded, or nonbonded. Each macrostate is an integral over corresponding microstates. The parameters of the model include<sup>55</sup> the energy of a perfect hydrogen bond,  $\epsilon_{\text{HB}}$ , the spring constant  $k_s$  for the angular variations of a hydrogen bond, the energy of a non-H-bonded vdW contact  $\epsilon_{\text{LJ}}$  and distance of contact  $\sigma_{\text{LJ}}$ , the diameter  $r_{\text{HB}}$  of a water molecule, the cooperativity energy  $\epsilon_c$ , mean-field attraction energy constant  $a$ , and weak hydrogen-bond volume parameter  $x_v$ . The model is nearly analytical. Its properties can be computed as functions of  $(T, p, N)$  in seconds on a single CPU. It shows how LJ attractions and repulsions are bal-

anced against hydrogen-bonding interactions differently at different temperatures and pressures. The theory reproduces volumetric properties such as the temperature of maximum density, the isothermal compressibility, the thermal expansion coefficient, and water's heat capacity in good agreement with the underlying MB model, which was previously studied by NPT Monte Carlo simulations, and in qualitative agreement with experimental trends. We find that applying pressure to water should reduce water's heat capacity which is consistent with works of Rebelo *et al.*<sup>84</sup> and Kumar *et al.*<sup>85</sup> Pressure also causes a negative thermal expansion coefficient at low temperature which is in agreement with experiments (below 4 C); see, for example, Ref. 86. We find that increased temperature increases the variance of H-bond angles and water's density. All these findings are consistent with experiments (Fig. 6 in Ref. 87) and with simulations for TIP4P water (Fig. 8 in Ref. 88). Increased pressure decreases the variance in density of our model which is in agreement with all the models cited above that show a decrease of  $\kappa_T$  with pressure, for example, Rebelo *et al.*<sup>84</sup> and Ref. 11 in their list.

## ACKNOWLEDGMENTS

We appreciate the support of the Slovenian Research Agency (Grant No. P1 0103-0201) and the NIH under Grant No. GM063592.

- <sup>1</sup>W. C. Röntgen, *Ann. Phys. Chem.* **45**, 91 (1892).
- <sup>2</sup>J. A. Pople, *Proc. R. Soc. London, Ser. A* **205**, 163 (1951).
- <sup>3</sup>G. M. Bell, *J. Phys. C* **5**, 889 (1972).
- <sup>4</sup>A. Rahman and F. H. Stillinger, *J. Chem. Phys.* **57**, 4009 (1972).
- <sup>5</sup>S. S. Borick, P. G. Debenedetti, and S. Sastry, *J. Phys. Chem.* **99**, 3781 (1995).
- <sup>6</sup>C. J. Roberts and P. G. Debenedetti, *J. Chem. Phys.* **105**, 658 (1996).
- <sup>7</sup>C. J. Roberts, A. Z. Panagiotopoulos, and P. G. Debenedetti, *Phys. Rev. Lett.* **77**, 4386 (1996).
- <sup>8</sup>N. A. M. Besseling and J. M. H. M. Scheutjens, *J. Phys. Chem.* **98**, 11597 (1994).
- <sup>9</sup>N. A. M. Besseling and J. Lyklema, *J. Phys. Chem.* **98**, 11610 (1994).
- <sup>10</sup>C. A. Angell, *J. Phys. Chem.* **75**, 3698 (1971).
- <sup>11</sup>G. Franzese, M. I. Marque, and H. E. Stanley, *Phys. Rev. E* **67**, 011103 (2003).
- <sup>12</sup>G. Némethy and H. A. Scheraga, *J. Chem. Phys.* **36**, 3382 (1962).
- <sup>13</sup>A. T. Hagler, H. A. Scheraga, and G. Némethy, *J. Phys. Chem.* **76**, 3229 (1972).
- <sup>14</sup>C. H. Cho, S. Singh, and G. W. Robinson, *Phys. Rev. Lett.* **76**, 1651 (1996).
- <sup>15</sup>T. M. Truskett, P. G. Debenedetti, S. Sastry, and S. Torquato, *J. Chem. Phys.* **111**, 2647 (1999).
- <sup>16</sup>G. Franzese, G. Malescio, A. Skibinsky, S. V. Buldyrev, and H. E. Stanley, *Nature (London)* **409**, 692 (2001).
- <sup>17</sup>G. Franzese, *J. Mol. Liq.* **136**, 267 (2007).
- <sup>18</sup>L. Pratt and D. Chandler, *J. Chem. Phys.* **73**, 3430 (1980).
- <sup>19</sup>G. Hummer, S. Garde, A. E. Garcia, M. E. Paulaitis, and L. R. Pratt, *J. Phys. Chem. B* **102**, 10469 (1998).
- <sup>20</sup>G. Hummer, S. Garde, A. E. Garcia, A. Pohorille, and L. R. Pratt, *Proc. Natl. Acad. Sci. U.S.A.* **93**, 8951 (1996).
- <sup>21</sup>J. A. Barker and R. O. Watts, *Chem. Phys. Lett.* **3**, 144 (1969).
- <sup>22</sup>A. Rahman and F. H. Stillinger, *J. Chem. Phys.* **55**, 3336 (1971).
- <sup>23</sup>F. H. Stillinger and A. Rahman, *J. Chem. Phys.* **60**, 1545 (1974).
- <sup>24</sup>H. J. C. Berendsen, J. P. M. Postma, W. F. van Gunsteren, and J. Hermans, in *Intermolecular Forces*, edited by B. Pullman (Reidel, Dordrecht, 1981), pp. 331–342.
- <sup>25</sup>W. L. Jorgensen, J. Chandrasekhar, J. D. Madura, R. W. Impey, and M. L. Klein, *J. Chem. Phys.* **79**, 926 (1983).
- <sup>26</sup>H. J. C. Berendsen, J. R. Grigera, and T. P. Straatsma, *J. Phys. Chem.* **91**, 6269 (1987).
- <sup>27</sup>M. W. Mahoney and W. L. Jorgensen, *J. Chem. Phys.* **112**, 8910 (2000).
- <sup>28</sup>H. W. Horn, W. C. Swope, J. W. Pitera, J. D. Madura, T. J. Dick, G. L. Hura, and T. Head-Gordon, *J. Chem. Phys.* **120**, 9665 (2004).
- <sup>29</sup>J. Caldwell, L. X. Dang, and P. A. Kollman, *J. Am. Chem. Soc.* **112**, 9144 (1990).
- <sup>30</sup>S. W. Rick, S. J. Stuart, and B. J. Berne, *J. Phys. Chem.* **101**, 6141 (1994).
- <sup>31</sup>H. Yu, T. Hansson, and W. F. van Gunsteren, *J. Chem. Phys.* **118**, 221 (2003).
- <sup>32</sup>P. Ren and J. W. Ponder, *J. Phys. Chem. B* **107**, 5933 (2003).
- <sup>33</sup>I.-F. W. Kuo and C. J. Mundy, *Science* **303**, 658 (2004).
- <sup>34</sup>A. G. Donchev, N. G. Galkin, A. A. Illarionov, O. V. Khoruzhii, M. A. Olevanov, M. V. Subbotin, and V. I. Tarasov, *Proc. Natl. Acad. Sci. U.S.A.* **103**, 8613 (2006).
- <sup>35</sup>R. Bukowski, K. Szalewicz, G. C. Groenenboom, and A. van der Avoird, *Science* **315**, 1249 (2007).
- <sup>36</sup>M. Patra and M. Karttunen, *J. Comput. Chem.* **25**, 678 (2004).
- <sup>37</sup>B. Hess, C. Holm, and N. van der Vegt, *J. Chem. Phys.* **124**, 164509 (2006).
- <sup>38</sup>P. Auffinger, T. E. Cheatham, and A. C. Vaiana, *J. Chem. Theory Comput.* **3**, 1851 (2007).
- <sup>39</sup>A. A. Chen and R. V. Pappu, *J. Phys. Chem. B* **111**, 11884 (2007).
- <sup>40</sup>J. M. Castillo, D. Dubbeldam, T. J. H. Vlugt, B. Smit, and S. Calero, *Mol. Simul.* **35**, 1067 (2009).
- <sup>41</sup>Y. V. Kalyuzhnyi, I. A. Protsykevitch, and P. T. Cummings, *Condens. Matter Phys.* **10**, 553 (2007).
- <sup>42</sup>S. Sastry, P. G. Debenedetti, F. Sciortino, and H. E. Stanley, *Phys. Rev. E* **53**, 6144 (1996).
- <sup>43</sup>H. Tanaka, *Europhys. Lett.* **50**, 340 (2000).
- <sup>44</sup>G. Franzese and H. E. Stanley, *J. Phys.: Condens. Matter* **14**, 2201 (2002).
- <sup>45</sup>C. J. Fennell and J. D. Gezelter, *J. Chem. Theory Comput.* **1**, 662 (2005).
- <sup>46</sup>L. A. Báez and P. Clancy, *J. Chem. Phys.* **103**, 9744 (1995).
- <sup>47</sup>M. Yamada, S. Mossa, H. E. Stanley, and F. Sciortino, *Phys. Rev. Lett.* **88**, 195701 (2002).
- <sup>48</sup>E. Sanz, C. Vega, J. L. F. Abascal, and L. G. MacDowell, *Phys. Rev. Lett.* **92**, 255701 (2004).
- <sup>49</sup>J. L. F. Abascal, E. Sanz, R. G. Fernández, and C. Vega, *J. Chem. Phys.* **122**, 234511 (2005).
- <sup>50</sup>J. L. F. Abascal and C. Vega, *J. Chem. Phys.* **123**, 234505 (2005).
- <sup>51</sup>T. Róg, K. Murzyn, J. Milhau, M. Karttunen, and M. Pasenkiewicz-Gierula, *J. Phys. Chem. B* **113**, 2378 (2009).
- <sup>52</sup>A. Ben-Naim, *J. Chem. Phys.* **54**, 3682 (1971).
- <sup>53</sup>A. Ben-Naim, *Mol. Phys.* **24**, 705 (1972).
- <sup>54</sup>G. Andolaro and R. M. Sperandio-Mineo, *Eur. J. Phys.* **11**, 275 (1990).
- <sup>55</sup>K. A. T. Silverstein, A. D. J. Haymet, and K. A. Dill, *J. Am. Chem. Soc.* **120**, 3166 (1998).
- <sup>56</sup>K. A. T. Silverstein, K. A. Dill, and A. D. J. Haymet, *Fluid Phase Equilib.* **120**, 3166 (1998).
- <sup>57</sup>N. T. Southall and K. A. Dill, *J. Phys. Chem. B* **104**, 1326 (2000).
- <sup>58</sup>K. A. T. Silverstein, A. D. J. Haymet, and K. A. Dill, *J. Chem. Phys.* **114**, 6303 (2001).
- <sup>59</sup>B. Hribar, N. T. Southall, V. Vlachy, and K. A. Dill, *J. Am. Chem. Soc.* **124**, 12302 (2002).
- <sup>60</sup>T. Urbič, V. Vlachy, Yu. V. Kalyuzhnyi, N. T. Southall, and K. A. Dill, *J. Chem. Phys.* **112**, 2843 (2000).
- <sup>61</sup>T. Urbič, V. Vlachy, Yu. V. Kalyuzhnyi, N. T. Southall, and K. A. Dill, *J. Chem. Phys.* **116**, 723 (2002).
- <sup>62</sup>T. Urbič, V. Vlachy, Yu. V. Kalyuzhnyi, and K. A. Dill, *J. Chem. Phys.* **118**, 5516 (2003).
- <sup>63</sup>T. Urbic, V. Vlachy, O. Pizio, and K. A. Dill, *J. Mol. Liq.* **112**, 71 (2004).
- <sup>64</sup>T. Urbic, V. Vlachy, Yu. V. Kalyuzhnyi, and K. A. Dill, *J. Chem. Phys.* **127**, 174505 (2007).
- <sup>65</sup>T. Urbic, V. Vlachy, Yu. V. Kalyuzhnyi, and K. A. Dill, *J. Chem. Phys.* **127**, 174511 (2007).
- <sup>66</sup>M. S. Wertheim, *J. Stat. Phys.* **42**, 477 (1986).
- <sup>67</sup>M. S. Wertheim, *J. Chem. Phys.* **87**, 7323 (1987).
- <sup>68</sup>A. Bizjak, T. Urbic, V. Vlachy, and K. A. Dill, *Acta Chim. Slov.* **54**, 532 (2007).
- <sup>69</sup>A. Bizjak, T. Urbic, V. Vlachy, and K. A. Dill, *J. Chem. Phys.* **131**, 194504 (2009).
- <sup>70</sup>C. L. Dias, T. Ala-Nissila, M. Grant, and M. Karttunen, *J. Chem. Phys.* **131**, 054505 (2009).
- <sup>71</sup>T. M. Truskett and K. A. Dill, *J. Chem. Phys.* **117**, 5101 (2002).

- <sup>72</sup>T. M. Truskett and K. A. Dill, *J. Phys. Chem. B* **106**, 11829 (2002).
- <sup>73</sup>K. A. Dill, T. M. Truskett, V. Vlachy, and B. Hribar-Lee, *Annu. Rev. Biophys. Biomol. Struct.* **34**, 173 (2005).
- <sup>74</sup>D. Eisenberg and W. Kauzmann, *The Structure and Properties of Water* (Oxford University Press, Oxford, 1969).
- <sup>75</sup>E. A. Jagla, *J. Chem. Phys.* **111**, 8980 (1999).
- <sup>76</sup>C. Huang, K. T. Wikfeldt, T. Tokushime, D. Nordlund, Y. Harada, U. Bergmann, M. Niebuhr, T. M. Weiss, Y. Horikawa, M. Leetmaa, M. P. Ljungberg, O. Takahashi, A. Lenz, L. Ojamae, A. P. Lyubartsev, S. Shin, L. G. M. Pettersson, and A. Nilsson, *Proc. Natl. Acad. Sci. U.S.A.* **106**, 15214 (2009).
- <sup>77</sup>G. Franzese and H. E. Stanley, *J. Phys.: Condens. Matter* **19**, 205126 (2007).
- <sup>78</sup>W. A. P. Luck, *J. Mol. Struct.* **448**, 131 (1998).
- <sup>79</sup>D. A. Fuentesvilla and M. A. Anisimov, *Phys. Rev. Lett.* **97**, 195702 (2006).
- <sup>80</sup>P. G. Debenedetti, *J. Phys.: Condens. Matter* **15**, R1669 (2003).
- <sup>81</sup>D. H. Bowman, C. Lim, and R. A. Aziz, *Can. J. Chem.* **46**, 1175 (1968).
- <sup>82</sup>L. Dordain, J.-Y. Coxam, J. R. Quint, J.-P. E. Grolier, E. W. Lemmon, and S. G. Penoncello, *J. Supercrit. Fluids* **8**, 228 (1995).
- <sup>83</sup>A. R. Henn and W. Kauzmann, *J. Phys. Chem.* **93**, 3770 (1989).
- <sup>84</sup>L. P. N. Rebelo, P. G. Debenedetti, and S. Sastry, *J. Chem. Phys.* **109**, 626 (1998).
- <sup>85</sup>P. Kumar, G. Franzese, and H. E. Stanley, *Phys. Rev. Lett.* **100**, 105701 (2008).
- <sup>86</sup>F. Mallamace, *Proc. Natl. Acad. Sci. U.S.A.* **106**, 15097 (2009).
- <sup>87</sup>M. A. Ricci, F. Bruni, and A. Giuliani, *Faraday Discuss.* **141**, 347 (2009).
- <sup>88</sup>P. Gallo and M. Rovere, *Phys. Rev. E* **76**, 061202 (2007).